Springer

KSME

Journal of Mechanical Science and Technology 30 (10) (2016) 4571~4578
www.springerlink.com/content/1738-494x(Print)/1976-3824(Online)
DOI 10.1007/s12206-016-0928-5

Measurement of unsteady transition on a pitching airfoil using dynamic pressure sensors †

Yongwei Gao, Qiliang Zhu and Long Wang*

School of Aeronautics, Northwestern Polytechnical University, Xi'an, 710072, China

(Manuscript Received November 17, 2015; Revised April 6, 2016; Accepted May 24, 2016)

Abstract

Unsteady boundary layer transition on a pitching OA209 airfoil in a wind tunnel was detected by using pressure fluctuation measurement at different oscillation frequency. Thirty Kulite dynamic pressure transducers flush-mounted on the airfoil surface recorded pressure signatures, and root mean square of pressure signatures were calculated. Results indicated that the criterion of transition for static airfoil defined as the peak of root mean square of pressure fluctuation was still suitable for detection of transition on a pitching airfoil. Fixed transition experiment for pitching airfoil was performed to validate the conclusion. Effect of oscillation frequency on transition was investigated. For small reduced frequency, the hysteresis loop is larger near leading edge. With increasing in the oscillation frequencies, the transition was promoted and relaminarization was enhanced.

Keywords: Pressure fluctuation; Pitching airfoil; Transition detection; Wind tunnel experiment

1. Introduction

Helicopter rotor blades, wind turbines, jet engine compressor blades, and aircraft maneuverability and so on generally involve aerodynamic characteristics of pitching airfoil. The aerodynamic unsteadiness of pitching oscillation airfoil should be carefully investigated. However, today's airfoil design methodologies still rely on steady computations and design criteria [1].

Some calculations about pitching airfoil or axial pump flow do not consider the effect of unsteady boundary layer events on performance [2, 3]. It is necessary to further take into account unsteady aerodynamic effects and characteristics of the airfoil in the design process.

However, unsteady boundary layer properties, such as laminar boundary layer separation, laminar reattachment, transition, relaminarization, and turbulent boundary layer separation, are rather complicated, and to a great extent depend on experimental measurements. Among the unsteady boundary layer properties, boundary layer transition/relaminarization gets more attention. Boundary layer transition generally results from a series of events, including instable waves, intermittent turbulent eddies, continuous turbulent eddies accompanied by increase in intermittency, sharp increase and rapid drop in turbulent intensity, and finally followed by fully-developed turbulence. In the meantime, increases in boundary layer thickness, surface temperature, wall shear stress and total pressure become observable. Because the exact location of transition is somewhat ambiguous, it is often convenient to define the peak of root mean square of temperature or pressure as indication of flow transition. Based on the transition characteristics, a variety of experimental techniques have been developed to detect the flow transition location.

Conventional hot-wire indirectly measures the heat transfer, and therefore the flow velocity, from a sensing element. Hot wire method has been widely applied for detection of transition. Early in the 1970s, Knapp et al. [4] and Lagraff [5] utilized the hot wire method to investigate subsonic and hypersonic boundary layer transition.

The method of Temperature sensitive paints (TSP) is an effective optical technique for measuring non-intrusively the surface temperature. The technique is based on the quenching of luminescent molecules that are sensitive to the local temperature. Costantini et al. [6] investigated the effects of non-adiabatic surface on transition measurements using temperature-sensitive paints. Fey et al. [7] using TSP detected transition at high Reynolds number in cryogenic wind tunnels. Borovoy et al. [8] studied boundary layer transition in short-duration wind tunnels by TSP method.

Infrared thermography that records infrared energy emitted from the model, and therefore temperature distribution on the model, can be used to determine the Stanton number in different surface regions (low level for laminar flow and high level

*Corresponding author. Tel.: +86 18092420475
E-mail address: onelong@nwpu.edu.cn
† Recommended by Associate Editor Seongwon Kang

for turbulent flow). Giepman et al. [9] measured boundary-layer transition front in supersonic flow by the method. An alternative based on infrared thermography is differential infrared thermography, which records the surface temperature's difference between regions of laminar and turbulent boundary layer flow, and therefore determines the transition location. Raffel et al. [10, 11] and Merz et al. [12] applied the method to detect the boundary layer transition on pitching NACA0012 airfoil.

Hot-film technique recognizes the state of boundary layer by measuring variation of heat transfer or voltage out level of hot-film sensors. Hodson et al. [13] and Zhang et al. [14] further defined the quasi-wall-shear stress by relation of output voltage of hot-film to wall shear stress. Lee et al. [15, 16] investigated the characteristic of unsteady boundary layer and stall events on an oscillating NACA 0012 airfoil by using closely spaced multiple hot-film sensor. Richter et al. [17] studied the unsteady transition characteristics of airfoil EDI-M109 by hot film technique. Kim et al. [18] investigated Reynolds number effects on unsteady boundary layer for oscillating NACA0012 airfoil with the aid of hot film and smoke-wire visualization. Haghiri et al. [19] studied the compressible influence on unsteady boundary layer using hot-film sensors.

Flow visualization methods, such as oil film interferometry [20] and smoke-wire method [21], are often rather useful for transition detection with combination of the aforementioned techniques.

Even so, it is still necessary to seek a convenient, effective and practical transition detection method for unsteady aerodynamics. Hot wire anemometry is intrusive and provides only point-wise flow information. Temperature sensitive paints should coat the model before experiment. Infrared thermography and hot film sensors seem too complicated. But above all, these techniques are not convenient for flight tests or practical flow control.

Compared with the above experimental techniques, it is more convenient and practical for pressure transducers to detect the boundary layer transition. Heller [22] using acoustic technique detected flow transition on hypersonic re-entry vehicles. Lewis and Banner [23], by using surface-pressure-fluctuation measurements, investigated the boundary layer transition on the X-15 vertical fin. With the progress of technology of pressure transducer manufacture, the transducer rapid response and miniaturization have been improved greatly. The pressure transducer measurement technique for steady flow transition detection has now been applied to a wide velocity range from low-speed flow to hypersonic in wind tunnel experiment.

In general for static airfoil experiment, if there are laminar, transition and turbulent flow zones, the position of peak of Root-mean-square (RMS) of pressure is thought of as the zone of transition. However, little investigation is available of unsteady boundary transition on a pitching airfoil by using pressure signature. Because of its successful application to static airfoil, it is fairly straightforward to reasonably consider applying pressure transducer measure technique to pitching oscillation airfoil. In the present paper, we performed an experiment on transition for pitching airfoil to demonstrate the feasibility, and it would be helpful for understanding unsteady flow transition and other unsteady boundary layer events.

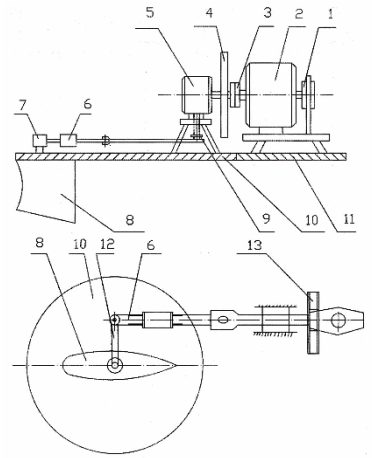

Fig. 1. Slider-crank oscillation system.

2. Arrangement of experiment

The testing was carried out in the NF-3 open-return type of low speed wind tunnel at Northwestern Polytechnical University, Xi'an, China. The NF-3 wind tunnel has three interchangeable test sections. The test section for airfoil testing is 8.0 m long and its cross section is rectangle, 1.60 m width by 3.0 m height. The maximum wind speed is 130 m/s and turbulence intensity is 0.045% in NF-3 wind tunnel.

The test model of airfoil OA209 used in the experiment was vertically installed between two turntables to adjust angle of attack. The test model was made of wood with steel skeleton inside, 600 mm chord length, 1600 mm span and 9% relative thickness. The airfoil pitch axis was located at 1/4–chord throughout experiment. Nominal angle of attack angle was measured by angle sensor mounted on the pitch axis. The angle sensor was produced by HEIDENHAIN, Germany, with resolution of ±5″. The model was driven by slider-crank mechanism as displayed in Fig. 1 in a sinusoidal motion of $\alpha = 10^{\circ}\sin(2\pi ft)$, where f is oscillation frequency.

Thirty dynamic differential pressure transducers (XCQ-093) produced by Kulite, Inc, America, were arranged on the upper and lower side of the airfoil as displayed in Fig. 2. The diameter of the cylindrical probe of the sensor was 2.4 mm. These transducers were embedded in the test model, and the surface of the pressure probe was flush with the model surface. Numbering these transducers was in clockwise direction from 1 to 30, starting at the leading edge. Before being installed, these transducers were calibrated on the ground by using Mensor CPC 6000 pressure controller.

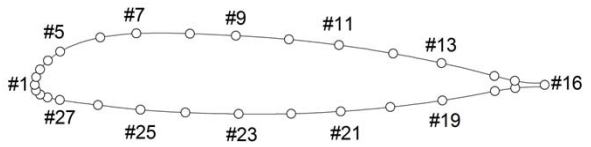

Fig. 2. Position and number of pressure transducers flush-mounted on the airfoil of OA209.

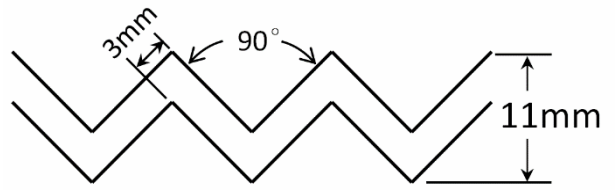

Fig. 3. ZZR type transition trip. The height was 0.35 mm.

Agilent VXI system with 32 phases (E8401A) accomplished the dynamic data acquisition. The acquisition speed was 100 KHz/phase, acquisition frequency was 0~20 kHz, acquisition accuracy was 0.1%, and the preset cut-off frequency of acquisition system was 20 kHz, which filters the frequency higher than 20 kHz.

Both static and oscillating airfoil experiments were performed for detection of transition. In the case of static airfoil, the experimental wind speeds were V = 20, 25, 30, 35, 40 m/s, the angle of attack was fixed at 4^o and the corresponding Reynolds numbers were Re = 0.8, 1.0, 1.2, 1.4, 1.6×10^6, respectively. For the purpose of comparison, another static test was conducted at $\alpha = 0^o$, 1^o, 2^o, 3^o and 4^o with fixed wind speed 30 m/s. In the case of oscillating airfoil, the wind speed was 30 m/s, the mean angle of attack was $\alpha = 0^o$, oscillation amplitude was 10^o, oscillation frequencies were f = 0.1, 0.2, 0.5 Hz, and the corresponding reduced frequencies $k = 2\pi fc/V$ were 0.013, 0.025, 0.063. Free transition experiment in wind tunnel was carried out for both the static and oscillating airfoil. To further validate the results on free transition in dynamic test, an extra fixed transition test was performed. Throughout the fixed transition wind tunnel experiment, a zigzag transition trip of type ZZR (Fig. 3) was adhered to the upper surface of airfoil at x/c = 0.05. The trip was 0.35 mm high.

3. Results and discussion

3.1 Static airfoil

In the case of the static airfoil test, the VXI system acquired the real-time signals of these 30 transducers with the acquisition frequency of 10 kHz and the acquisition time of 20 s. And then, the signals of each transducer at the same angle of attack were averaged to obtain corresponding pressure distribution on the airfoil surface.

Fig. 4 presents the pressure distributions at $\alpha = 4°$ for different wind speeds and Fig. 5 displays the pressure distribution at 30 m/s wind speed for different angles of attack. Both pressure distributions demonstrate the flow on the upper surface is attached.

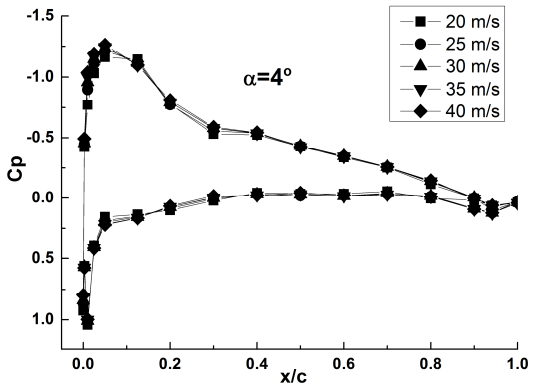

Fig. 4. Pressure distributions at different wind speeds.

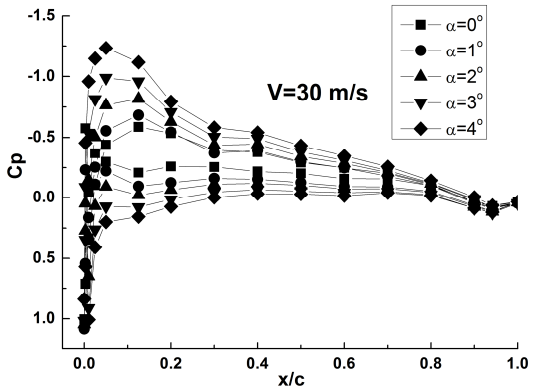

Fig. 5. Pressure distributions at different angles of attack.

The Root-mean-square (RMS) value of pressure fluctuation can be used to detect the transition location. Although the pressure fluctuation in the turbulent flow is larger than that in the laminar flow, the maximum of pressure fluctuation occurs in transition flow, which is called the transition peak. Based on the knowledge, the root-mean-square value of pressure fluctuation on the upper surface was applied to detect the position of the transition peak, therefore the transition position. The normalized RMS of surface pressure fluctuation for different wind speed at fixed angle of attack of 4^o is shown in Fig. 6. The transition position moves forward with increasing wind speed. At a wind speed of 20 m/s and 25 m/s, the transition position is located at x/c = 0.2 and moves forward to x/c = 0.125 at wind speed of 30 m/s, 35 m/s and 40 m/s, which is in accord with the observation that the increasing Reynolds number brings the transition forward. However, the sparse distribution of transducers cannot distinguish the subtle and sensitive transition variations between wind speeds of 30 m/s, 35 m/s and 40 m/s.

Fig. 7 displays the variation of transition position with angle of attack at fixed wind speed of 30 m/s. At $\alpha = 0°$, 1°, 2°, the position of normalized RMS peak value is x/c = 0.3, then moves forward to x/c = 0.2 at $\alpha = 3°$, and further forward to x/c = 0.125 at $\alpha = 4°$. Within static stall angle, the higher the angle of attack is, the more forward the transition position moves.

The detailed surface pressure fluctuations at locations x/c =

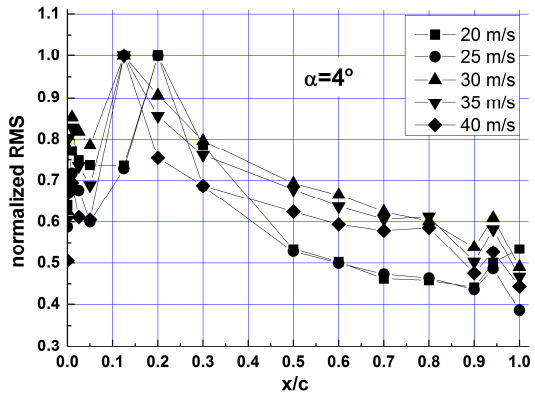

Fig. 6. Normalized RMS of surface pressure fluctuation at different wind speeds for static airfoil.

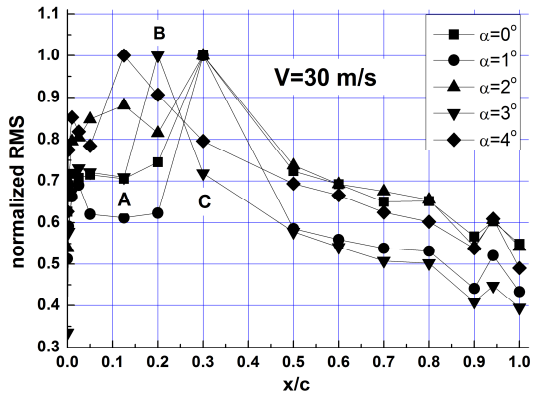

Fig. 7. Normalized RMS of surface pressure fluctuation at different angles of attack for static airfoil.

0.125 (A), 0.2 (B) and 0.3(C) for static airfoil at $\alpha = 3°$ are displayed in Fig. 8. The location B corresponds to the position of transition peak. The location A is within the laminar region and location C is within the turbulent region. The signature at A, B and C reflects the relative intensity of pressure fluctuation. The fluctuation intensity at location B reaches the maximum level, which indicates transition event occurs in the surface flow.

Fig. 9 shows power spectral density for pressure fluctuations at the three locations. The power spectral density tells the difference more clearly. At transition region x/c = 0.2, higher frequencies are activated. Moreover, Fig. 9 indicates that the fluctuation intensity behind transition (x/c = 0.3) drops to a still significant level but higher than the fluctuation intensity before transition (x/c = 0.125).

Variation of transition position with angle of attack and wind speed are displayed in Figs. 10 and 11. For the purpose of comparison, XFOIL is used to calculate the transition position at the same conditions. XFOIL was first developed by Prof. Mark Drela at MIT as a design tool for the MIT Daedalus project in the 1980s. It can predict the transition by e^N method. Here, N = 8 was taken. Increasing in either wind speed or angle of attack leads to the forward movement of transition position, which complies with the general knowledge of boundary transition, though the not-closely-spaced distribution of dynamic pressure transducers at leading edge in the present testing cannot accurately detect the variation of transition point at smaller angle of attack. The result from static airfoil indicates that the operation of the wind tunnel, model, transducers and apparatuses in this experiment was well-conditioned and has established the foundation of proceeding with the oscillating airfoil experiment.

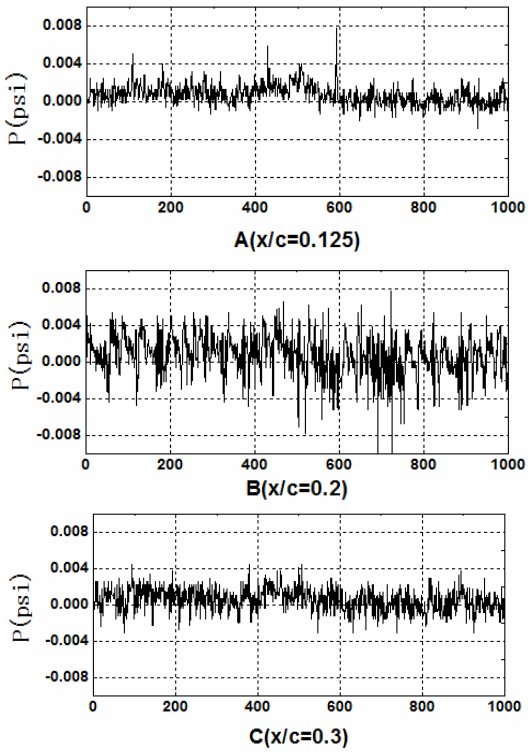

Fig. 8. Surface pressure fluctuations at locations A (x/c = 0.125), B(x/c = 0.2) and C(x/c = 0.3) for static airfoil at $\alpha = 3°$.

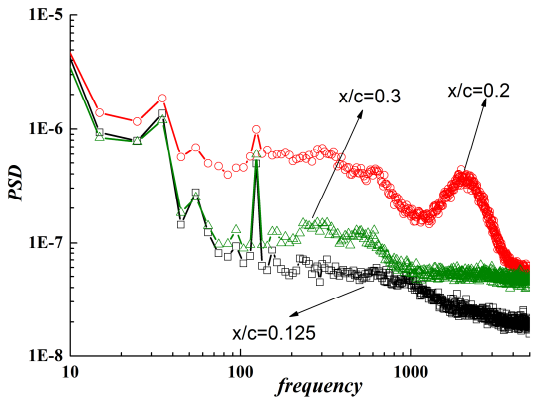

Fig. 9. Power spectral density for pressure fluctuation at locations A, B and C.

3.2 Oscillating airfoil

3.2.1 Data processing

The wind speed in the case of oscillating airfoil was 30 m/s,

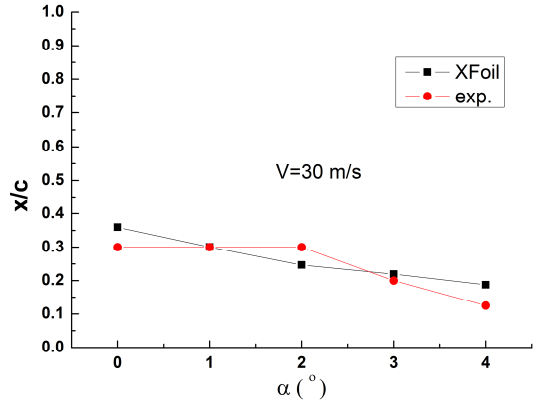

Fig. 10. Variation of transition position with wind speed.

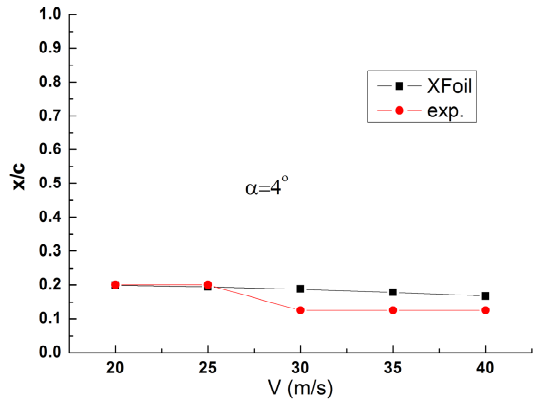

Fig. 11. Variation of transition position with angle of attack.

acquisition frequency was 500 Hz, oscillation frequencies of the model were f = 0.1, 0.2, and 0.5 Hz, respectively, and the corresponding acquisition times were 1280 s, 1280 s, and 1024 s.

Phase-averaged method is often applied in the processing data from pitching airfoil. Data with the same phase is used to calculate the variation of average value and root mean square of signature with phase. Large amount of data is needed for accurate statistic values. It is important for phase-averaged method to keep the strict periodicity of oscillation system. However, as a result of the clearance error between mechanical part and motor driven system, the points of data acquired during different oscillation period are not strictly identical (e.g., while oscillation frequency was 0.1 Hz, 5077 data points were in the 1st period, but 5012 data points in the 2nd with 65 points missing, and as well the similar situation existed in the latter period), and thus the data statistic of each period according to the acquisition points or time became rather complex. Furthermore, due to the inertia, when the airfoil pitched to the maximum amplitude, the angle of attack would have slight fluctuation and the measured angles were irregular. If large storage capacity of acquisition system is available, one can pick up the data with the same phase or angle to get accurate statistic result. However, practical limitation of storage capacity made it more difficult to process imperfectly sampled dynamic data.

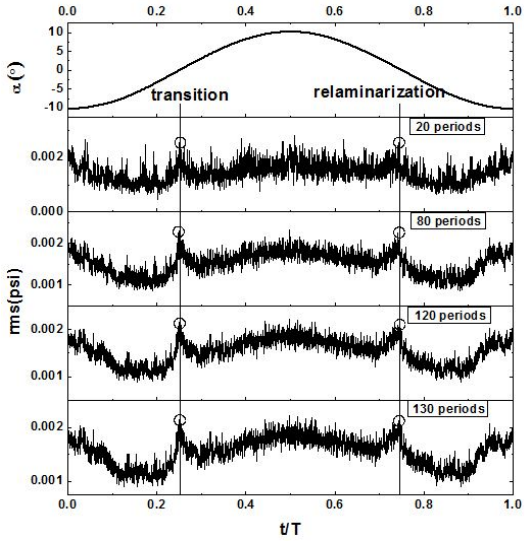

Fig. 12. Variation of RMS with number of sample periods for phase averaged method. Sampling position was located at x/c = 0.3. The RMS peak gradually emerged with the increase in number of sampling periods.

A fitted phase-averaged method was put forward in the present paper to obtain the reliable statistical values. First, the ascending 0° point was labeled as the initial point, and the time between two consecutive ascending 0° points was regarded as a period. Then, the same number of data were obtained from every period by first-order interpolation. Finally, the fitted data with the same phase were collected together to calculate the mean value and Root mean square (RMS) in a normalized period as the following:

$$RMS(t_i)=\sqrt{\frac{1}{n}\sum_{k=0}^{n-1}\left(p(t_i+kT)-\overline{p}_i\right)^2}\,, \tag{1}$$

where

$$\overline{p}_i=\frac{1}{n}\sum_{k=0}^{n-1}p(t_i+kT)\,, \tag{2}$$

was phase-averaged pressure, T was oscillation period, and n the number of sampling periods.

In the present study, the number of interpolation points in a period was 3000. As mentioned, the RMS peak of pressure signature determined the transition position, and therefore it was key to find a sharp RMS peak. However, as far as the phase-averaged method is concerned, the sharp RMS peak depended on the number of sampling periods. Fig. 12 displays the variation of RMS of pressure signature at x/c = 0.3 with number of sampling periods, while oscillating frequency was 0.2 Hz. Too few sampling periods, e.g., 20 periods, could not clearly tell the RMS peak. With the increase in the number of sampling periods, the RMS peak gradually emerged. We adopted 120 sampling periods to find the sharp RMS peak.

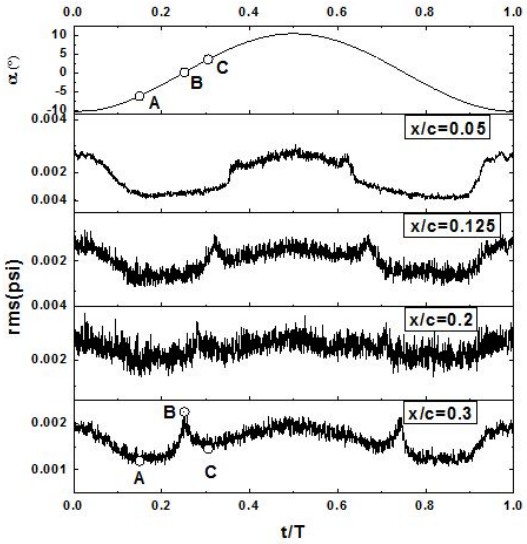

Fig. 13. Free transition case: RMS value of pressure fluctuation on oscillating OA209 airfoil at x/c = 0.05, 0.125, 0.2, 0.3.

3.2.2 Oscillation at frequency 0.2 Hz

The RMS value of pressure fluctuation for free transition at oscillation frequency 0.2 Hz is presented in Fig. 13. The transition peaks in Fig. 13 are obvious. The transition peak first occurs at x/c = 0.3 at $\alpha \approx 0°$. And then pitching up motion moves the transition peak to x/c = 0.2 at $\alpha \approx 1.9°$. Further pitching up shifts the transition peak forward to x/c = 0.125 at $\alpha \approx 4.4°$. At $\alpha \approx 6.6°$, the location of transition peak approaches x/c = 0.05, almost at the leading edge. The RMS level behind transition peak is higher than before the transition peak, which means flow in the turbulent state. In the motion of pitching down, there occurs another RMS peak, which indicates flow relaminarization. Relaminarization first occurs at x/c = 0.05, and further pitching down moves the relaminarization downstream.

At the bottom of Fig. 13, the labels A, B and C represent three different flow states. The original pressures signatures corresponding to the flow states A, B and C are presented in Fig. 14. Fig. 14(a) displays the pressure fluctuation in the laminar flow, Fig. 14(b) in the transitional flow, and Fig. 14(c) in the turbulent flow. As in the case of static airfoil, Fig. 14 indicates that pressure fluctuation in transition state is still maximum for pitching airfoil, and thus the transition peak is easy to identify. By a comparison of the results in static experiments with that in pitching airfoil experiments, one can draw the conclusion that the transition peak detected from RMS value of pressure fluctuation can determine the transition position both for static and pitching airfoil.

The variation of transition and relaminarization position with angle of attack is presented in Fig. 15, which only displays the transition or relaminarization positions detected by pressure transducers at x/c = 0.05, 0.125, 0.2, 0.3 and 0.4 on the upper airfoil surface. Beyond x/c = 0.4, the flow is always turbulent. The reduced frequency $k = 0.013$ is so low that the

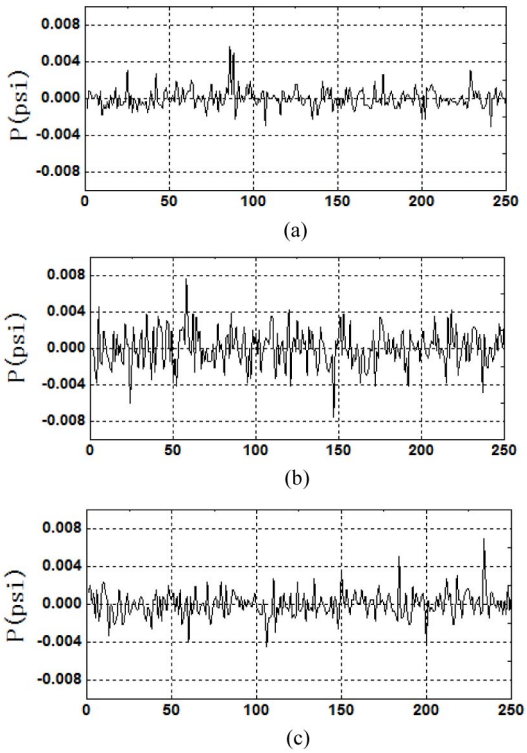

Fig. 14. Variation of pressure fluctuation with time at x/c = 0.3.

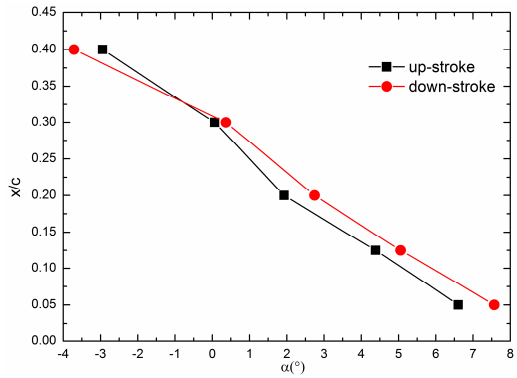

Fig. 15. Transition and relaminarization position on the upper surface for pitching OA209 airfoil at wind speed of 30 m/s and oscillation frequency of 0.2 Hz.

hysteresis loop is small. At $\alpha \approx -1°$, the upstroke curve (laminar flow transition) and downstroke curve (turbulent flow relaminarization) cross. At angles of attack above $\alpha \approx -1°$, as far as fixed chord position is concerned, e.g., x/c = 0.2, the relaminarization angle is larger than the transition angle; thus downstroke motion is favorable for flow relaminarization. While angle of attack is below $\alpha \approx -1°$, the upstroke motion causes the enhancement of laminarity. However, for small oscillation frequency, e.g., 0.2 Hz, one can roughly say that transition during upstroke and relaminarization during downstroke almost occur at the same angle of attack.

To further verify the feasibility of pressure RMS method for pitching airfoil, a fixed transition experiment, in which transi-

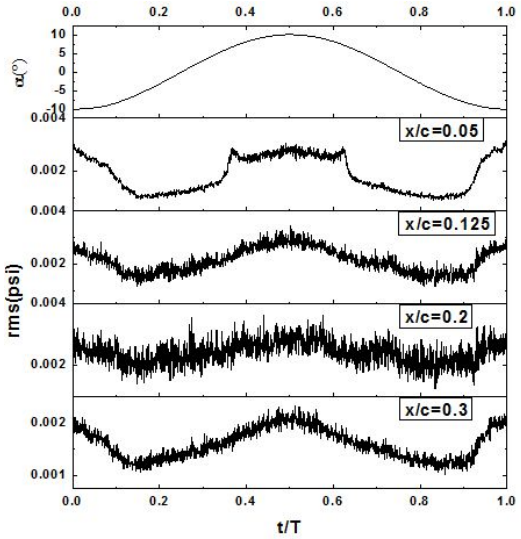

Fig. 16. Fixed transition case: RMS value of pressure fluctuation on oscillating OA209 airfoil at x/c = 0.05, 0.125, 0.2 and 0.3.

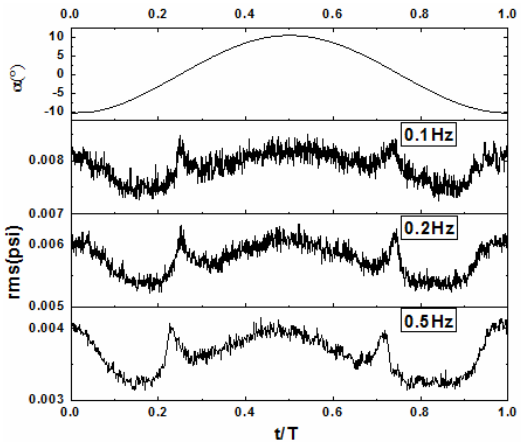

Fig. 17. Variation of RMS value at x/c = 0.3 for different oscillation frequency.

tion trip was fixed at x/c = 0.05, was performed. Fig. 6 displays RMS value of pressure fluctuation at x/c = 0.05, 0.125, 0.2, and 0.3 in the fixed transition case. The transition peaks evident in the free transition case, as shown in Fig. 13, however, were only recognized at x/c = 0.05 (before transition trip) in the fixed transition case. As for at x/c = 0.125 and the latter positions, no transition peak of RMS occurred, i.e., the boundary-layer flow already had changed to turbulence. The fixed transition experiment for oscillation airfoil further demonstrated that occurrence of the transition peak was a characteristic feature of flow transition no matter whether static or pitching airfoil experiment was performed.

3.2.3 Effect of oscillation frequency on transition peak

The effect of oscillation frequency on transition peak was investigated in the present paper. The investigation was carried out at V = 30 m/s and oscillation frequency of 0.1, 0.2, and 0.5 Hz. Fig. 17 presents RMS value of pressure fluctuation at x/c = 0.3 for different oscillation frequency. During the upstroke motion, the transition angle at x/c = 0.3 is 0.47° for oscillation frequency of 0.1 Hz, 0.065° for 0.2 Hz and -1.39° for 0.5 Hz. During the downstroke motion, the relaminarization angle at x/c = 0.3 is 0.46° for frequency of 0.1 Hz, 0.37° for 0.2 Hz and 1.56° for 0.5 Hz. With the increase in oscillation frequency, the transition is promoted and relaminarization is enhanced.

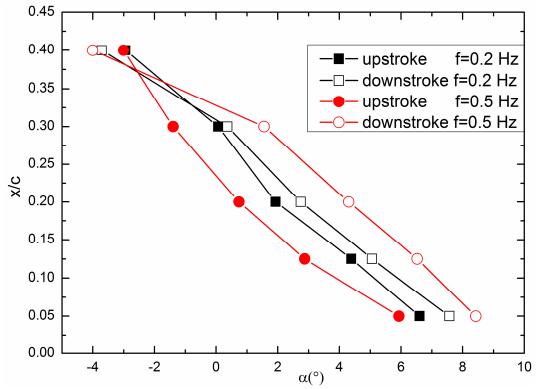

Fig. 18. Hysteresis loops for transition peak at oscillation frequencies of 0.2 and 0.5 Hz.

The hysteresis loops for transition peak at oscillation frequencies of 0.2 Hz and 0.5 Hz are presented in Fig. 18. With increasing in oscillation frequency, the hysteresis loop is larger near the leading edge and basically encircles the small hysteresis loop. Note that in the present study the oscillation frequency is lower and in the case of higher oscillation frequency the hysteresis loop for transition peak is larger at the most downstream position [17].

4. Conclusions

Experiments on transition detection by using RMS peak of surface pressure fluctuation were performed for static and pitching OA209 airfoil in wind tunnel. The RMS peak was manifest for either static or pitching airfoil. Results indicated that transition position on pitching airfoil could be detected by finding RMS peak of fluctuated pressure signature. Experiments on fixed transition for pitching airfoil demonstrated the conclusion. Moreover, effect of low oscillation frequency on transition peak has been investigated especially. At low oscillation frequency, e.g., k = 0.013, the hysteresis loop for the transition peak was small. With increasing in oscillation frequency, the hysteresis loop became larger and encircled the small hysteresis loop. In contrast to higher frequency pitching, upstroke motion at low frequency promoted the laminar flow transition, and downstroke motion at low frequency enhanced turbulent flow relaminarization.

Acknowledgment

Authors thank Bin-Bin Wei, Jia-Peng Zhang and other staff in the NF-3 lab for their help in the wind tunnel experiment.

Nomenclature

C_p : Pressure coefficient
P_i : Pressure
PSD : Power spectral density
RMS : Root mean square
V : Wind velocity
α : Angle of attack

References

[1] A. Klein et al., Unsteady criteria for rotor blade airfoil design, *35th European Rotorcraft Forum*, Hamburg, Germany (2009).

[2] M. R. Mohaghegh and M. M. Jafarian, Periodic transonic flow simulation using fourier-based algorithm, *J. of Mechanical Science and Technology*, 28 (10) (2014) 4109-4119.

[3] J. Feng, X. Luo, P. Guo and G. Wu, Influence of tip clearance on pressure fluctuations in an axial flow pump, *J. of Mechanical Science and Technology*, 30 (4) (2016) 1603-1610.

[4] C. F. Knapp and P. J. Roache, A combined visual and hot-wire anemometer investigation of boundary-layer transition, *AIAA J.*, 6 (1) (1968) 29-36.

[5] J. E. Lagraff, Observations of hypersonic boundary-layer transition using hot wire anemometry, *AIAA J.*, 10 (6) (1972) 762-769.

[6] M. Costantini et al., Nonadiabatic surface effects on transition measurements using temperature sensitive paints, *AIAA Journal*, 53 (5) (2015) 1172-1187.

[7] U. Fey, Y. Egami and C. Klein, Temperature-sensitive paint application in cryogenic wind tunnels: Transition detection at high reynolds numbers and influence of the technique on measured aerodynamic coefficients, *22nd International Congress on Instrumentation in Aerospace Simulation Facilities*, California, USA (2007) 304-320.

[8] V. Borovoy et al., Temperature sensitive paint application for investigation of boundary layer transition in short-duration wind tunnels, *Progress in Flight Physics*, 3 (2012) 15-24.

[9] R. H. M. Giepman, F. F. J. Schrijer and B. W. van Oudheusden, Infrared thermography measurements on a moving boundary-layer transition front in supersonic flow, *AIAA J.*, 53 (7) (2015) 2056-2061.

[10] M. Raffel and C. B. Merz, Differential infrared thermography for unsteady boundary-layer transition measurements, *AIAA J.*, 52 (9) (2014) 2090-2093.

[11] M. Raffel et al., Differential infrared thermography for boundary layer transition detection on pitching rotor blade models, *Experiments in Fluids*, 56 (2) (2015) 1-13.

[12] C. B. Merz, K. Richter and M. Raffel, Unsteady boundary layer transition measurements by differential infrared thermography, *70th Annual Forum of the American Helicopter Society,* Quebec, Canada (2014).

[13] H. Hodson and R. Howell, Unsteady flow: Its role in the low pressure turbine, *9th International Symposium Unsteady Aerodynamics, Aeroacoustics and Aeroelasticity of Turbomachine,* Lyon, France (2000).

[14] X. Zhang, M. Ali and S. Steen, Hot-film measurements of boundary layer transition, separation and reattachment on a low-pressure turbine airfoil at low reynolds numbers, *38th AIAA/ASME/SAE/ASEE Joint Propulsion Conference & Exhibit*, Indiana, USA (2002) 3643-3655.

[15] T. Lee and P. Gerontakos, Investigation of flow over an oscillating airfoil, *J. of Fluid Mechanics,* 512 (2004) 313-341.

[16] T. Lee and S. Basu, Measurement of unsteady boundary layer developed on an oscillating airfoil using multiple hot-film sensors, *Experiments in Fluids*, 25 (2) (1998) 108-117.

[17] K. Richter et al., Experimental investigation of unsteady transition on a pitching rotor blade airfoil, *J. of the American Helicopter Society*, 59 (1) (2014) 1-12.

[18] D. H. Kim and J. W. Chang, Reynolds number effects on unsteady boundary layer for an oscillating airfoil, *27th AIAA Applied Aerodynamics Conference,* San Antonio, Texas, USA (2009) 3501-3513.

[19] A. Haghiri, M. Mani and N. Fallahpour, Unsteady boundary layer measurement on an oscillating (pitching) supercritical airfoil in compressible flow using multiple hot-film sensors, *J. of Aerospace Engineering*, 229 (10) (2015) 1771-1784.

[20] E. Schülein, H. Rosemann and S. Schaber, Transition detection and skin friction measurements on rotating propeller blades, *28th AIAA Aerodynamic Measurement Technology, Ground Testing and Flight Testing Conference*, New Orleans, LA, USA (2012) 3202-3226.

[21] S. M. Batill and T. J. Mueller, Visualization of transition in the flow over an airfoil using the smoke-wire technique, *AIAA J.*, 19 (3) (1981) 340-345.

[22] H. H. Heller, Acoustic technique for detection of flow transition on hypersonic re-entry vehicles, *AIAA J.*, 7 (12) (1969) 2227-2232.

[23] T. L. Lewis and R. D. Banner, Boundary layer transition detection on the x-15 vertical fin using surface-pressure-fluctuation measurements, *NASA TM X-2466* (1971).

Yongwei Gao received his Bachelor's in aerodynamics, and Master's and Ph.D. in fluid dynamics from Northwestern Polytechnical University (NPU) in China. He is a Professor at the school of Aeronautics and head of the laboratory of NF-3 low-speed wind tunnel in NPU. His works focus on experimental fluid dynamics and aero acoustics.